receiving clean waveforms and transmitting waveforms with fast rise/fall times. Inputs and outputs were terminated to ground with 50Ω and 100Ω on-chip resistors, respectively. The power supply voltage was −3·5 V.

Fabrication: The IC was fabricated using the 0·2 μm-gate-length SAINT (self-aligned implantation for N^+ layer technology) process [6] based on conventional optical lithography and ion implantation for easy adaptation to commercial products. The typical cutoff frequency for the 0·2 μm FET was 50 GHz and the transconductance was 400 mS/mm.

IC performance: The IC was tested on the wafer with RF probes. In the measurement the IC was fed differential clock inputs with a DC bias of −2·2 V. The T-F/F operation was measured by observing the output signal at (CK/2). The operation of the T-F/F was stable up to 20 GHz, about 30% faster than a conventional IC fabricated with the same process. The self-oscillation of the T-F/F was 15 GHz. These operation results show very good agreement with simulation.

The MUX operation was confirmed using a 10 Gbit/s PN pattern generator and an error detector. Two low-speed pseudorandom signals from the PN pattern generator were combined into a single high-speed signal by the MUX. The original two signals were regenerated with a MESFET D-F/F IC [7] and checked with the error detector.

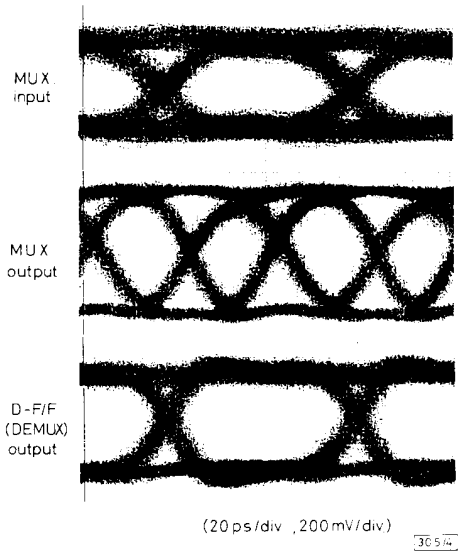

Fig. 4 *Operating waveforms of MUX at 20 Gbit/s*

Fig. 4 shows the operating waveforms of the MUX at 20 Gbit/s. The output signals show good eye opening and a sufficient peak-to-peak voltage of more than 1 V. Fig. 5 shows the input sensitivity and phase margin of the MUX. The input sensitivity of the MUX at 20 Gbit/s was 720 mV and the phase margin was over 200 degrees. The power dissipation was 3·4 W.

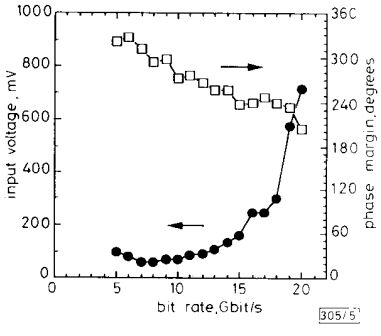

Fig. 5 *Input sensitivity and phase margin of MUX*

Conclusion: A 20 Gbit/s MUX has been developed using 0·2 μm-gate-length MESFETs with a cutoff frequency of 50 GHz. The high operating speed was achieved owing to a novel static T-F/F, which operated stably up to 20 GHz. The operating speed of the MUX is about 70% faster than that previously reported for two-bit MUXs using MESFETs of a similar cutoff frequency.

Acknowledgment: We should like to thank Dr. K. Hagimoto for making this work possible, and Dr. N. Ieda and Dr. S. Horiguchi for their continual encouragement throughout this work.

8th September 1992

K. Murata, M. Ohhata, M. Togashi and M. Suzuki (*NTT LSI Laboratories, 3-1, Morinosato Wakamiya, Atsugi-shi, Kanagawa Pref., 243-01 Japan*)

References

1 RUNGE, K., DANIEL, D., and GIMLETT, J. L.: 'A 27 Gb/s AlGaAs/GaAs HBT 4 : 1 multiplexer IC'. IEEE GaAs IC symposium, 1991, pp. 233–236

2 ISHIDA, K., WAKIMOTO, H., YOSHIHARA, K., KONNO, M., SHIMIZU, S., UCHITOMI, N., and TOYODA, N.: '12 Gbps GaAs 2-bit multiplexer/demultiplexer chip set for the SONET STS-192 system'. IEEE GaAs IC symposium, 1989, pp. 317–320

3 REIN, H.-M., HAUENSCHILD, J., MÖLLER, M., MCFARLAND, W., PETTENGILL, D., and DOERNBERG, J.: '30 Gbit/s multiplexer and demultiplexer ICs in silicon bipolar technology', *Electron. Lett.*, 1992, **28**, pp. 97–99

4 OHHATA, M., YAMANE, Y., ENOKI, T., SUGETA, S., KATO, N., and HIRAYAMA, M.: '11 Gbit/s multiplexer and demultiplexer using 0·15 μm GaAs MESFETs', *Electron. Lett.*, 1990, **26**, (7), pp. 467–468

5 TAKADA, T., and OHHATA, M.: 'A new interfacing method 'SCFL-interfacing' for ultra-high-speed logic ICs'. IEEE GaAs IC symposium, 1990, pp. 211–214

6 YAMANE, Y., OHHATA, M., KIKUCHI, H., ASAI, K., and IMAI, Y.: 'A 0·2 μm GaAs MESFET technology for 10 Gb/s digital and analog IC's'. IEEE MTT-S Digest, 1991, pp. 513–516

7 OHHATA, M., YAMANE, Y., ENOKI, T., SUGITANI, S., KATO, N., HAGIMOTO, K., and HIRAYAMA, M.: '13 Gbit/s D-type flip-flop IC using GaAs MESFETs', *Electron. Lett.*, 1990, **26**, (14), pp. 1039–1040

EFFECT OF FIXED EMISSION WAVELENGTH ON THRESHOLD CURRENT OF InGaAsP SEMICONDUCTOR LASER DIODES

J. O'Gorman and A. F. J. Levi

Indexing terms: Semiconductor lasers, Threshold current

The authors demonstrate and quantify the extent to which a reduced variation of laser diode threshold current with temperature can be achieved by fixing lasing wavelength on the long wavelength side of the room temperature gain peak. This enhancement ($T_0 = 92$ K) occurs at the expense of increased threshold current at low temperatures. Fixing the lasing wavelength on the short wavelength side of the room temperature gain peak to reduce dynamic spectral broadening occurring at high modulation rates leads to reduced T_0 (= 30 K) in comparison to Fabry-Perot laser diodes T_0 (= 42 K) made from the same material.

The choice of lasing wavelength for single mode, fixed wavelength, laser diodes, such as distributed feedback (DFB) or distributed Bragg reflector (DBR) structures, can have considerable impact on device performance. For example, it has been shown [1] that the linewidth enhancement factor and hence high-speed modulation performance of DFB lasers may be improved by detuning DFB gratings to the short wavelength side of the gain peak. On the other hand, T_0 in these

fixed wavelength semiconductor lasers can be enhanced artificially by detuning the emission wavelength to the long wavelength side of the gain peak [2, 3]. In this situation one is taking advantage of the shift of diode laser peak gain to longer wavelengths with increasing temperature. Determination of the useful limits of such detunings is the subject of this Letter.

We report results of experiments using a narrow linewidth, tunable external cavity laser (TECL) to investigate the influence of fixed feedback wavelength on temperature sensitivity of threshold current in InGaAsP laser diodes. We find that there is a dramatic improvement in T_0 when emission wavelength is tuned to the long wavelength side of the room temperature gain peak. On the other hand, T_0 decreases slowly as emission wavelength is detuned to the short wavelength side.

The devices used in our experiments are of a standard bulk active region InGaAsP buried heterostructure design. Similar results, however, were obtained with multiple quantum well lasers. The active region is a $0{\cdot}14\,\mu$m thick InGaAsP layer with band gap $\lambda_g = 1{\cdot}28\,\mu$m, lattice matched to an n-type InP substrate and capped by a p-type InP layer. After a two step regrowth process, the active region has width $w = 1\,\mu$m and is surrounded by index guiding InP. As-cleaved devices, of length $l = 260\,\mu$m, lase with wavelength $\lambda = 1{\cdot}31\,\mu$m and have threshold current $I_{th} = 8{\cdot}5$ mA at $T = 298$ K. The variation of lasing threshold current with temperature, when fitted to the phenomenological expression $I_{th} = I^0 \exp(T/T_0)$, yields $T_0 = 42$ K when averaged over the temperature range $20°C \leq T \leq 55°C$. Unless otherwise stated, all values of T_0 discussed in this letter are obtained in this temperature range.

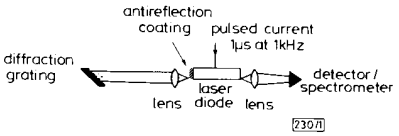

Fig. 1 *Schematic diagram of external cavity laser diode*

The grating feeds light back into the AR coated facet of the laser diode which is electrically pumped with current I

The experimental arrangement for our external cavity experiments is shown in Fig. 1. Light output from a high quality antireflection coated facet is efficiently coupled to the external cavity by a low loss lens. The tunable external cavity laser (TECL), of length $L_C \simeq 20$ cm, is closed by a 600 groove/mm diffraction grating. The laser emission may be tuned in a single instrument limited line ($<0{\cdot}15$ nm) across the semiconductor gain spectrum. When measuring laser threshold currents, in order to prevent increase in device temperature due to ohmic heating at high drive currents, the laser was driven with 1 μs pulses at a 1 kHz repetition rate. In initial experiments, however, we investigated the temperature dependence of lasing threshold current in an external cavity laser closed with a broad-band high reflectivity plane mirror. Both room temperature threshold current and its increase with increasing temperature were the same as for the uncoated device*. This fact shows that the optimum external cavity alignment may be reproducibly achieved even with change in heat-sink temperature. Consequently, with sufficient care, TECLs may be used to reliably measure the temperature dependence of laser diode threshold current where the wavelength of maximum feedback occurs in a narrow spectral region under the gain curve. It is not necessary to examine large numbers of different discrete devices with the attendant risk of possible sample dependent anomalies.

We investigated the temperature dependence of TECL threshold current for different emission wavelengths. For modest bias currents around room temperature ($I \lesssim 30$ mA) the TECL exhibited a large tuning range of about 100 nm while preserving a narrow instrument limited spectral line. TECL threshold currents were measured for $1{\cdot}24\,\mu m \leq \lambda \leq 1{\cdot}34\,\mu$m in 10 nm intervals for the temperature range, $20°C \leq T \leq 82°C$. With increasing temperature, this wavelength tuning range decreased due to the magnitude of current required to achieve threshold (and consequently carrier pinning by superluminescence) at the extremes of the tuning range. At $T = 82°C$ the tunable wavelength range was $1{\cdot}27\,\mu m \leq \lambda \leq 1{\cdot}355\,\mu$m.

In Fig. 2 we show laser threshold current variation with wavelength for seven temperatures lying in the range $20°C \leq T \leq 82°C$. At each temperature, threshold current increases rapidly with increased detuning from the gain peak (i.e. wavelength of minimum threshold). This occurs because carrier density must be increased to bring net gain at the detuned wavelength above the total cavity loss level. The strong asymmetry of the laser gain spectrum together with a shift in peak gain to shorter wavelengths with increasing carrier density causes lasing threshold to increase more rapidly with tuning to longer wavelengths.

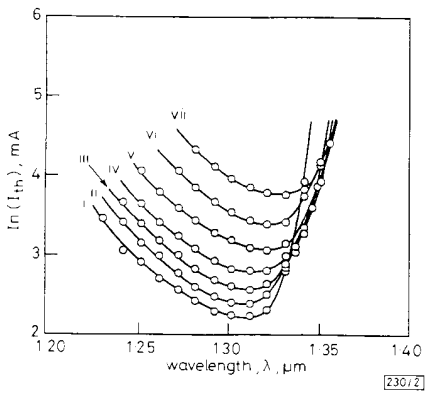

Fig. 2 *Natural logarithm of measured laser threshold current I_{th} as a function of wavelength λ for various temperatures*

(i) $T = 20{\cdot}6°C$
(ii) $T = 28{\cdot}1°C$
(iii) $T = 35{\cdot}6°C$
(iv) $T = 43{\cdot}3°C$
(v) $T = 54{\cdot}0°C$
(vi) $T = 69{\cdot}0°C$
(vii) $T = 81{\cdot}8°C$

Fig. 3 is a semilogarithmic plot of TECL threshold current variation with temperature for various emission wavelengths in the cavity tuning range. For $\lambda = 1{\cdot}25\,\mu$m on the short wavelength side of the room temperature gain peak a low $T_0 = 30$ K is observed. For $\lambda = 1{\cdot}33\,\mu$m however, a wavelength detuned to the long wavelength side of the room temperature peak gain wavelength, an impressively large $T_0 = 92$ K is observed.

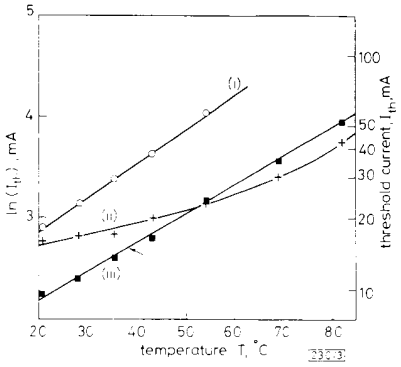

Fig. 3 *Natural logarithm of measured TECL threshold current as a function of temperature for various emission wavelengths*

(i) $T_0 = 30$ K $\lambda = 1{\cdot}25\,\mu$m
(ii) $T_0 = 92$ K $\lambda = 1{\cdot}33\,\mu$m
(iii) $T_0 = 35$ K $\lambda = 1{\cdot}30\,\mu$m

* O'GORMAN, J., and LEVI, A. F. J.: 'Wavelength dependence of T_0 in InGaAsP semiconductor laser diodes', (unpublished)

In Fig. 4 we plot the variation of T_0 as a function of fixed lasing emission wavelength. The solid curve shows T_0 obtained in the temperature range $20°C \leq T \leq 52°C$ and the broken curve is for $20°C \leq T \leq 82°C$. Clearly, T_0 increases rapidly with detuning of feedback wavelength to the long wavelength side of the room temperature peak gain wavelength. This enhancement of T_0 is an artifact in the sense that no material factors have been improved. In addition, this increase in T_0 comes at the expense of the room temperature threshold current. Fig. 4 also shows that, due to the shift of semiconductor laser peak gain to longer wavelengths with increasing temperature, single mode, fixed wavelength lasers will show a reduced T_0 when emission wavelength is shortened to reduce dynamic spectral broadening.

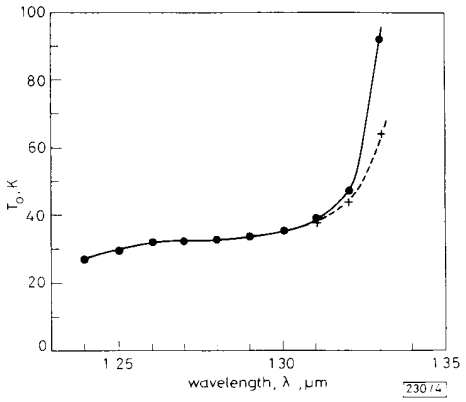

Fig. 4 *Measured variation of T_0 as a function of emission wavelength, λ*
The solid curve shows T_0 obtained in the temperature range $20°C \leq T \leq 55°C$ and the broken curve is for $20°C \leq T \leq 82°C$

In conclusion, we have demonstrated and quantified the extent to which a reduced variation of laser threshold current with temperature may be achieved by fixing lasing wavelength on the long wavelength side of the room temperature gain peak. This enhancement occurs at the expense of increased threshold current at low temperatures. Fixing the lasing wavelength on the short wavelength side of the room temperature gain peak to reduce dynamic spectral broadening occurring at high modulation rates leads to reduced $T_0 = 30\,K$ in comparison to Fabry-Perot laser diodes $T_0 = 42\,K$ made from the same material.

Acknowledgment: We thank E. J. Flynn for providing the devices used in this work and K. Wecht for antireflection coating the laser diodes.

1st September 1992

J. O'Gorman and A. F. J. Levi (*AT&T Bell Laboratories, Murray Hill, NJ 07974 USA*)

References

1 OGITA, S., YANO, N., ISHIKAWA, H., and IMAI, H.: 'Linewidth reduction in DFB laser by detuning effect', *Electron. Lett.*, 1987, **23**, pp. 393–394

2 TSANG, W. T., CHOA, F. S., LOGAN, R. A., TANBUN-EK, T., SERGENT, A. M., and WECHT, K. W.: 'Reduced temperature dependence of threshold current by broadband enhanced feedback: A new approach and demonstration', *Appl. Phys. Lett.*, 1992, **60**, pp. 18–20

3 TSANG, W. T., OLSSON, N. A., and LOGAN, R. A.: 'Threshold-wavelength and threshold-temperature dependences of GaInAsP/InP lasers with frequency selective feedback operating in the 1·3- and 1·5-μm regions', *Appl. Phys. Lett.*, 1983, **43**, pp. 154–156

SPEAKER ADAPTATION IN SPEECH RECOGNITION USING LINEAR REGRESSION TECHNIQUES

S. Cox

Indexing terms: Speech recognition, Linear regression techniques

A new technique of speaker adaptation for use in speaker-independent speech recognition systems is presented. The training data is used to build models (based on linear regression) of sounds. At recognition time, the models are used together with an incomplete set of sounds from a new speaker to estimate values for unheard sounds, which are used to adapt the speaker-independent models.

Introduction: Algorithms for speaker adaptation in speech recognition have usually concentrated on refining estimates of the system's speech model parameters after it has been exposed to vocabulary examples from a new speaker [1]. In most cases, when the system 'hears' an example of sound X from the new speaker it updates only the parameters of the model of X. In this Letter, our premise is that an example of the sound X from the new speaker contains potentially useful information about many speech sounds that that speaker is likely to produce, so that when the system hears an example of sound X from the new speaker, it updates parameters of several other models as well as the model for X. Adaptation of models of unheard sounds is achieved by first building linear regression models of each vocabulary sound using the training data and then, given an incomplete set of vocabulary sounds from a new speaker, using these models to predict values of unheard vocabulary sounds from the speaker. These predictions are then used to adapt the system model parameters.

Data and models: We have begun our experiments by using examples of individual vowels from different speakers because much of the interspeaker acoustic variation is contained within the vowels and using isolated vectors dispenses with the need for time alignment procedures. The data consisted of a single example of each of 11 vowels from each of 30 speakers (15 male, 15 female). Each (RP) speaker spoke the following /hVd/ words: heed, hoard, hid, hood, head, who'd, had, hudd, hard, heard, hod. The steady-state portion of each vowel was represented by a single 8-dimensional mel-frequency cepstral coefficient (MFCC) vector [2]. The dataset was divided into a training-set of speakers 1–16 (8 male, 8 female) and a test-set of speakers 17–30. Each vowel class was modelled as a multivariate Gaussian probability density with a mean equal to the training-set sample mean and with a common diagonal covariance matrix formed by averaging the sample covariance matrices of the classes. An example from the test-set was classified by computing its likelihood from each of the 11 probability densities.

Preliminary investigation: Fig. 1 shows scatterplots, for each of the 8 MFCC dimensions, of values of vowel no. 3 (x-axis) against values of vowel no. 8 (y-axis) for the 30 speakers in the data-set. The correlation coefficients for these plots are 0·86, 0·81, 0·91, 0·41, 0·84, 0·50, 0·76 and 0·63 in dimensions 1, 2, ..., 8, respectively. The mean correlation coefficient averaged over all vowel pairings in all 8 MFCC dimensions was 0·48, indicating that prediction of values using a linear regression model was viable.

Experimental method and baseline results:

(1) *Experimental method:* For each speaker within the test-set, the 11 vowel examples available were divided into 5 vowels to be used for the purposes of adaptation and the remaining 6 vowels for testing. To ensure a bias-free result, all 462 ways of choosing the 5 adaptation vowels and the 6 remaining test vowels were used for each speaker. The 5 adaptation vowels were used to predict values of the 6 unseen vowels and these predicted values were used to modify the estimate of the means for the corresponding 6 vowel classes. The modification was of the form new_mean = p * sample_mean + (1 − p) * predicted_value where $0 < p < 1$ (p is chosen empirically). The 6 unseen vowels (only) were then classified using the set of modified means and the result noted.